RSC Advances

PAPER

View Article Online
View Journal | View Issue

Cite this: *RSC Adv.*, 2024, **14**, 5846

Highly electron-deficient 1-propyl-3,5-dinitropyridinium: evaluation of electron-accepting ability and application as an oxidative quencher for metal complexes†

Akitaka Ito, *[ab] Yasuyuki Kuroda,[a] Kento Iwai, [ab] Soichi Yokoyama ‡[ab] and Nagatoshi Nishiwaki *[ab]

Received 2nd February 2024
Accepted 8th February 2024

DOI: 10.1039/d4ra00845f

rsc.li/rsc-advances

Impacts of the nitro groups on the electron-accepting and oxidizing abilities of *N*-propylpyridinium were evaluated quantitatively. A 3,5-dinitro derivative has efficiently quenched emission from photosensitizing Ru(II) and Ir(III) complexes owing to the thermodynamically-favored electron transfer to the pyridinium whose LUMO is greatly lowered by the presence of electron-withdrawing nitro groups.

Introduction

Pyridines are typical electron-deficient heterocyclic compounds that can be seen all around us as substructures of functional materials such as pharmaceuticals, ligands, and optical and electronic devices.[1] The nucleophilic ring nitrogen, furthermore, undergoes *N*-alkylation, resulting in pyridinium salt. Owing to their highly electron-deficient aromatic character, pyridinium skeletons have been utilized in a variety of natural/artificial systems as electron acceptors as represented by NAD^+,[2] methyl viologen[3] and so forth.[4] On the other hand, a nitro group exhibits strong electron-withdrawing ability due to both resonance and inductive effects, with the latter effect equivalent to two chloro groups.[5] Therefore, a combination of the highly electron-deficient pyridinium and strong electron-withdrawing nitro group is expected to significantly increase the oxidation or electron-accepting abilities.

In our previous work, we have demonstrated that 1-propyl-3,5-dinitropyridinium salt **2a**·OTs is formed *in situ* upon treatment of *N*-propyl-β-formyl-β-nitroenamine **1a** (R = Pr) with *p*-toluenesulfonic acid (TsOH), and formation of the salt **2a**·OTs is confirmed by trapping as 4-arylated 1,4-dihydropyridine derivatives **3** with electron-rich benzenes.[6] On the other hand, 3,5-dinitropyridine **4** was obtained when *N*-*tert*-butylenamine **1b** (R = *t*-Bu) was subjected to the same reaction, which is because a stable *tert*-butyl cation is readily eliminated (Scheme 1). The easy access to 3,5-dinitropyridine **4** facilitates the *N*-modification to afford versatile *N*-alkyl-3,5-dinitropyridinium salts **2**. Indeed, treatment of **4** with propyl triflate (PrOTf) proceeded at room temperature to furnish **2a**·OTf. This easily modifiable feature prompted us to evaluate the electron-acceptability of its *N*-alkylated form ($\mathbf{2a}^+$) by comparing with 3-nitro and unsubstituted pyridinium relatives ($\mathbf{5}^+$ and $\mathbf{6}^+$) that are prepared from commercially available pyridines by *N*-propylation.

Experimental

Preparation of 2a·OTf

A mixture of 3,5-dinitropyridine **4** (86 mg, 0.5 mmol) and PrOTf (122 mg, 0.63 mmol) was stirred without solvent at room temperature for 2 d. Colorless precipitates were collected and washed with CH_2Cl_2 to afford **2a**·OTf (95 mg, 0.28 mmol, 56%) as colorless powder, mp 217.0–217.8 °C. ^{1}H NMR (400 MHz, CD_3CN) δ 1.03 (t, J = 7.6 Hz, 3H), 2.12 (tq, J = 7.6, 7.6 Hz, 2H),

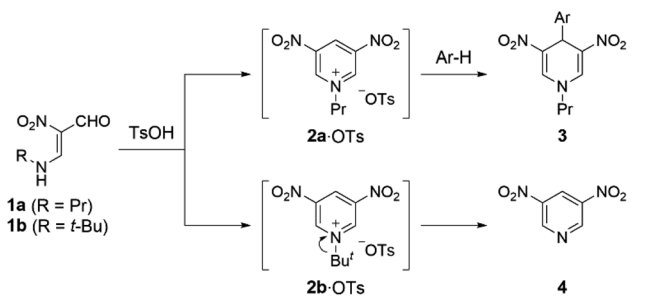

Scheme 1 Generation of 1-alkyl-3,5-dinitropyridinium salts **2**·OTs *in situ* from *N*-alkyl-β-formyl-β-nitroenamines **1**.

[a]*School of Engineering Science, Kochi University of Technology, Tosayamada, Kami, Kochi 782-8502, Japan. E-mail: ito.akitaka@kochi-tech.ac.jp, nishiwaki.nagatoshi@kochi-tech.ac.jp*

[b]*Research Center for Molecular Design, Kochi University of Technology, Tosayamada, Kami, Kochi 782-8502, Japan*

† Electronic supplementary information (ESI) available: Cyclic voltammograms of the metal complexes and emission quenching data by $\mathbf{5}^+$ and $\mathbf{6}^+$. See DOI: https://doi.org/10.1039/d4ra00845f

‡ Present address: The Institute of Scientific and Industrial Research (SANKEN), Osaka University, Ibaraki, Osaka 567-0047, Japan.

4.80 (t, J = 7.6 Hz, 2H), 9.78 (t, J = 2.0 Hz, 1H), 9.94 ppm (d, J = 2.0 Hz, 2H); ^{13}C NMR (100 MHz, CD_3CN) δ 10.2 (CH_3), 25.3 (CH_2), 66.5 (CH_2), 121.8 (q, J = 318.0 Hz, CF_3), 135.9 (CH), 147.3 (CH), 147.9 ppm (C); ^{19}F NMR (376 MHz, CD_3CN) δ 79.36 ppm; HRMS (ESI-TOF) calcd for $C_8H_{10}N_3O_4$ (M^+): 212.0666, found: 212.0676.

Characterization of 5·OTf

mp 102.3–102.7 °C. ^{1}H NMR (400 MHz, CD_3CN) δ 1.00 (t, J = 7.2 Hz, 3H), 2.06 (tq, J = 7.2, 7.2 Hz, 2H), 4.66 (t, J = 7.2 Hz, 2H), 8.30 (dd, J = 8.4 Hz, 6.2 HZ, 1H), 9.01 (dd, J = 6.2, 2.0 Hz, 1H), 9.18 (ddd, J = 8.4, 2.0, 1.2 Hz, 1H), 9.63 ppm (d, J = 1.2 Hz 1H); ^{13}C NMR (100 MHz, CD_3CN) δ 10.3 (CH_3), 25.2 (CH_2), 65.2 (CH2), 125.1 (q, J = 319 Hz, CF_3), 130.4 (CH), 141.0 (CH), 142.7 (CH), 147.8 (C), 150.1 ppm (CH); ^{19}F NMR (376 MHz, CD_3CN) δ 79.31 ppm; HRMS (ESI-TOF) calcd for $C_8H_{11}N_2O_2$ (M^+): 167.0815, found: 167.0819.

Characterization of 6·OTf

^{1}H NMR (400 MHz, CD_3CN) δ 1.00 (t, J = 7.6 Hz, 3H), 2.06 (tq, J = 7.6, 7.6 Hz, 2H), 4.49 (t, J = 7.6 Hz, 2H), 8.03 (br, 2H), 8.51 (t, J = 7.6 Hz, 1H), 8.70 ppm (d, J = 5.6 Hz, 2H); ^{13}C NMR (100 MHz, CD_3CN) δ 9.3 (CH_3), 24.0 (CH_2), 62.9 (CH_2), 120.9 (q, J = 318 Hz, CF_3), 128.1 (CH), 144.2 (CH), 145.5 ppm (CH); ^{19}F NMR (376 MHz, CD_3CN) δ 79.30 ppm; HRMS (ESI-TOF) calcd for $C_8H_{12}N$ (M^+): 122.0964, found: 122.0966.

Other chemicals

$[Ru(bpy)_3](PF_6)_2$ (bpy = 2,2′-bipyridine) is the same sample which has been used in the earlier literatures.[7] $[Ir(ppy)_2(bpy)]PF_6$ (ppyH = 2-phenylpyridine) was synthesized and purified similarly to the reported procedure.[8] Tetra-*n*-butylammonium hexafluorophosphate ($TBAPF_6$, Wako Pure Chemical Industries) was purified by repeated recrystallizations from ethanol. Ferrocene (Wako Pure Chemical Industries) was used as supplied. Anhydrous or spectroscopic-grade CH_3CN (Wako Pure Chemical Industries) was used without further purification for the electrochemical or spectroscopic measurements, respectively.

Electrochemical measurements

Cyclic voltammetry of the complexes in CH_3CN at 298 K was performed by using a BAS ALS-1202A electrochemical analyzer with a three-electrode system using glassy-carbon working, Ag auxiliary, and $Ag/AgNO_3$ reference electrodes (~0.01 mol dm^{-3} (=M) in CH_3CN containing ~0.1 M $TBAPF_6$) supplied by BAS Inc. The sample solutions containing a pyridinium salt or metal complex (~1.0 mM) and $TBAPF_6$ as a supporting electrolyte (~0.1 M) in the absence or presence of ferrocene as an internal standard were deaerated by purging an argon-gas stream over 20 min prior to measurements. The potential sweep rate was 100 mV s^{-1}.

Emission quenching study

Emission spectra were recorded and emission quantum yields (Φ_{em}) were determined by the absolute method using a Hamamatsu Photonics Quantaurus-QY Plus C13534-02. Emission intensity at each wavelength was corrected for system spectral response so that the vertical axis of a spectrum corresponds to the photon number at each wavelength. Emission decay profiles of $[Ir(ppy)_2(bpy)]PF_6$ was measured by using a Hamamatsu C4334 streak camera with a C5094 polychromator by exciting at 400 nm using second harmonics of a femtosecond-pulse mode-locked Ti:sapphire laser (MKS Instruments Spectra-Physics Tsunami® 3941-M1BB and 3980 frequency doubler/pulse selector, 1 MHz) and analyzed by a single exponential decay function. Sample solutions were deaerated by purging with an argon-gas stream for over 30 min.

Free energy changes for the electron-transfer processes ($-\Delta G$) were calculated by:[9]

$$-\Delta G = nF[E_{1/2}(Q^{+/0}) - E_{1/2}(M^*)] + Z_Q Z_M e^2/D_s d = nF[E_{1/2}(Q^{+/0}) - E_{1/2}(M)] + E_0(M^*) + Z_Q Z_M e^2/D_s d \quad (1)$$

In eqn (1), $E_{1/2}(Q^{+/0})$ is the reduction potential of Q^+, and $E_{1/2}(M)$ is the oxidation potential of the complex (1.32 and 1.63 V *vs.* SCE for $[Ru(bpy)_3]^{2+}$ and $[Ir(ppy)_2(bpy)]^+$, respectively, see Fig. S1†). $E_0(M^*)$ is the excited-state zeroth energy and has been determined to be 16 360 and 16 850 cm^{-1} for $[Ru(bpy)_3]^{2+}$ and $[Ir(ppy)_2(bpy)]^+$, respectively, by the Franck–Condon analysis.[10] Z_Q and Z_M are the charges of Q^+ and complex. d is the sum of effective radii of Q^+ and complex estimated for the optimized geometries by DFT calculations (4.7, 4.6, 4.4, 6.2 and 6.2 Å for **2a**$^+$, **5**$^+$, **6**$^+$, $[Ru(bpy)_3]^{2+}$ and $[Ir(ppy)_2(bpy)]^+$, respectively). D_s, n, F and e are the static dielectric constant of the solvent (relative dielectric constant of CH_3CN: 37.5), the number of electrons transferred, the Faraday constant and the formal charge, respectively. It should be noted that, in eqn (1), an electrostatic work term for the electron-transfer products was omitted since the reduced pyridiniums are charge-neutral.

Theoretical calculations

Theoretical calculations for the compounds were conducted with Gaussian 09W software (Revision C.01).[11] The ground-state geometries of the pyridinium cations were optimized by using density functional theory (DFT) using the restricted B3LYP functional with 6-31+G(d,p) basis set. All the optimized geometries did not gave any negative frequencies under identical methodologies. Lowest-energy unoccupied molecular orbitals were plotted using GaussView 5.[12] All the calculations were carried out as in acetonitrile by using a polarizable continuum model (PCM).

Results and discussion

Down-field shifts of the ring protons in the ^{1}H NMR spectra in CD_3CN were observed as the number of nitro groups increased (Fig. 1), indicating a decrease in the electron density of the pyridine ring. All the pyridiniums **2a**$^+$, **5**$^+$ and **6**$^+$ in CH_3CN exhibited an irreversible reduction wave as shown in Fig. 2. Half reduction potential ($E_{1/2}$) was shifted to a positive potential region with increasing the nitro group ($E_{1/2}$ = −0.061 (**2a**$^+$), −0.41 (**5**$^+$) and −0.80 V (**6**$^+$) *vs.* saturated calomel electrode

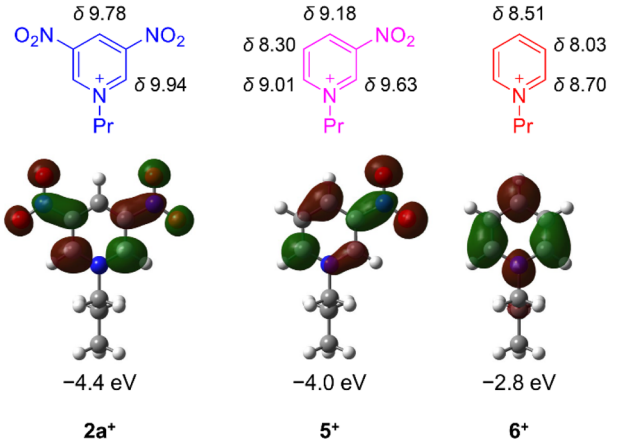

Fig. 1 Chemical shifts of ^{1}H NMR in CD_3CN (given in ppm) and LUMO distributions/energies of pyridiniums $\mathbf{2a}^+$, $\mathbf{5}^+$ and $\mathbf{6}^+$.

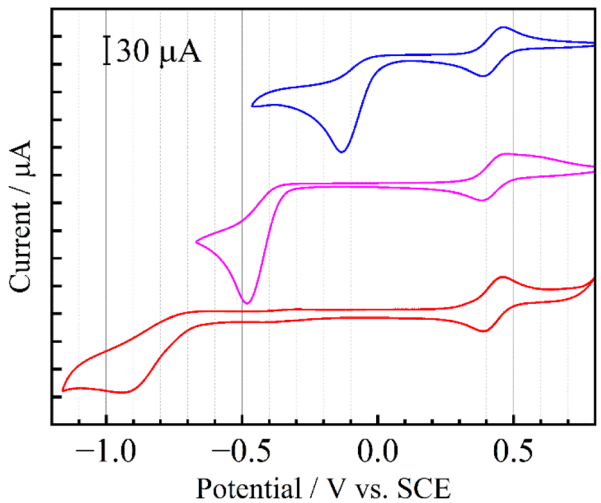

Fig. 2 Cyclic voltammograms of **2a**·OTf (blue), **5**·OTf (pink) and **6**·OTf (red) in deaerated CH_3CN containing 0.1 M $TBAPF_6$. Reversible waves at around +0.43 V represent redox couples of ferrocene as an internal standard.

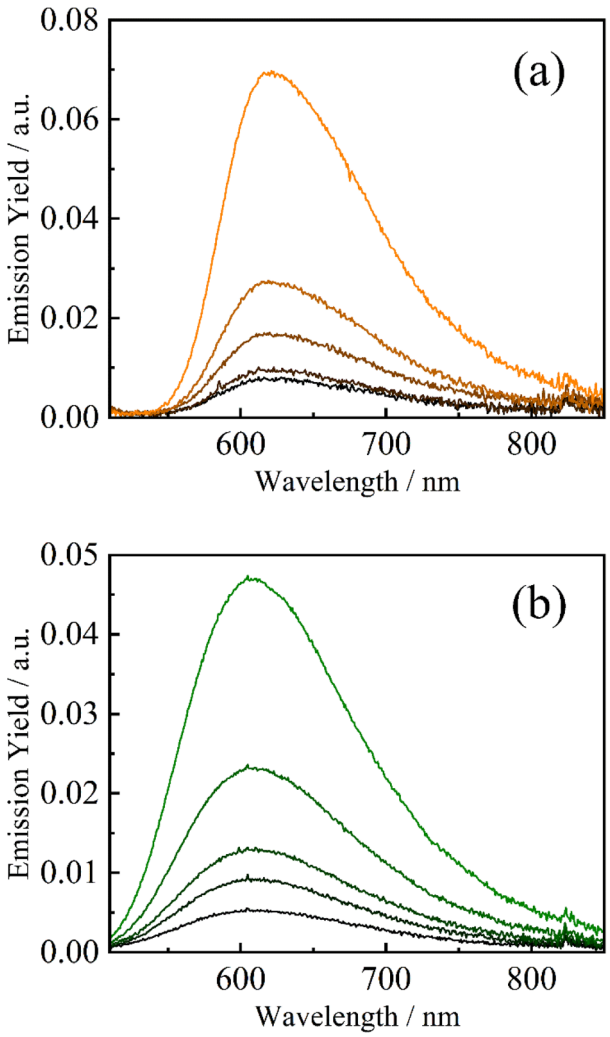

Fig. 3 Emission spectra of $[Ru(bpy)_3](PF_6)_2$ (a, 3.8×10^{-5} M, $\lambda_{ex} = 500$ nm) and $[Ir(ppy)_2(bpy)]PF_6$ (b, 3.8×10^{-4} M, $\lambda_{ex} = 470$ nm) in the absence and presence of dinitropyridinium salt **2a**·OTf ($(0.0–4.0) \times 10^{-3}$ M: orange/green → black) in deaerated CH_3CN.

(SCE)). These tendencies were supported by DFT calculations, as the LUMO energy of $\mathbf{2a}^+$ was lowered to −4.4 eV (see Fig. 1). It is, furthermore, worth emphasizing that the $E_{1/2}$ value of $\mathbf{2a}^+$ is surprisingly positive even by comparing with that of methyl viologen (−0.44 V *vs.* sodium saturated calomel electrode (SSCE)[13]). In contrast to fully reversible redox behavior of methyl viologen and resulting applications as a redox shuttle,[3] the highly-positive reduction potential of $\mathbf{2}^+$ is advantageously utilizable as a sacrificial electron acceptor in the various photochemical systems.

The strong electron-accepting ability of $\mathbf{2a}^+$ is utilizable as an oxidative quencher in photoinduced electron-transfer reactions. As shown in Fig. 3(a), emission from a famous photosensitizer $[Ru(bpy)_3]^{2+}$ (ref. 14) in CH_3CN (3.8×10^{-5} M) was reduced upon addition of $\mathbf{2a}^+$ ($(0.0–4.0) \times 10^{-3}$ M), and emission quantum yield (Φ_{em}) of $[Ru(bpy)_3]^{2+}$ was decreased from 0.096 to 0.014 in the presence of $\mathbf{2a}^+$ (4.0×10^{-3} M). Emission from a cyclometalated iridium(III) complex $[Ir(ppy)_2(bpy)]^+$ in CH_3CN (3.8×10^{-4} M) was also quenched when $\mathbf{2a}^+$ coexisted in a solution ($\Phi_{em} = 0.085$ and 0.017 in the absence and presence (4.0×10^{-3} M) of $\mathbf{2a}^+$, respectively) as shown in Fig. 3(b). Stern–Volmer plots for emission quenching of the complexes by $\mathbf{2a}^+$ are shown in Fig. 4, together with those by $\mathbf{5}^+$ and $\mathbf{6}^+$ (emission spectra are shown in Fig. S2–S5†). The plots exhibited good linear dependences, irrespective of the complex and pyridinium, as expressed by the Stern–Volmer equation: $\Phi_{em,0}/\Phi_{em} = 1 + k_q\tau_0[Q^+]$ with $\Phi_{em,0}$ and Φ_{em} the emission quantum yields in the absence and presence of the quencher (*i.e.*, $\mathbf{2a}^+$, $\mathbf{5}^+$ or $\mathbf{6}^+$), respectively, k_q the quenching rate constant, τ_0 the excited-state lifetime of the complex in the absence of the quencher (890 and 300 ns for $[Ru(bpy)_3]^{2+}$ [15] and $[Ir(ppy)_2(bpy)]^+$, respectively), and $[Q^+]$ the quencher concentration. As clearly seen in Fig. 4 and Table 1, emission quenching by $\mathbf{2a}^+$ ($k_q = 1.6 \times 10^9$ and 3.2×10^9 M^{-1} s^{-1} for $[Ru(bpy)_3]^{2+}$ and $[Ir(ppy)_2(bpy)]^+$, respectively)

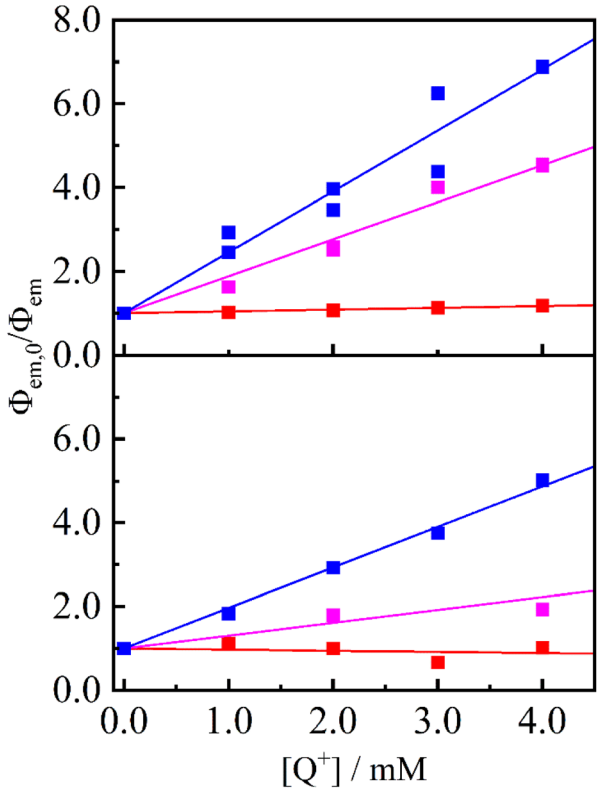

Fig. 4 Stem–Volmer plots for $[Ru(bpy)_3]^{2+}$ (top panel) and $[Ir(ppy)_2(bpy)]^+$ (bottom panel) quenching by $\mathbf{2a}^+$ (blue), $\mathbf{5}^+$ (pink) and $\mathbf{6}^+$ (red) in deaerated CH_3CN. Solid lines represent linear regressions with the intercept fixed at **1**.

Table 1 Reduction potentials, driving forces for electron transfer and quenching rate constants of pyridiniums $\mathbf{2a}^+$, $\mathbf{5}^+$ and $\mathbf{6}^+$

		$[Ru(bpy)_3]^{2+}$		$[Ir(ppy)_2(bpy)]^+$	
Q^+	$E_{1/2}$/V	$-\Delta G$/eV	$k_q/10^9$ M^{-1} s^{-1}	$-\Delta G$/eV	$k_q/10^9$ M^{-1} s^{-1}
$\mathbf{2a}^+$	−0.061	+0.72	1.6	+0.43	3.2
$\mathbf{5}^+$	−0.41	+0.37	0.99	+0.084	1.0
$\mathbf{6}^+$	−0.80	+0.016	0.048	−0.30	<0.01

was more efficient than those by $\mathbf{5}^+$ and $\mathbf{6}^+$ ($k_q \leq 1.0 \times 10^9$ M^{-1} s^{-1}), indicating that the more nitro group, the stronger the quenching ability.

The efficient emission quenching by $\mathbf{2a}^+$ can be discussed in terms of a driving force of the electron-transfer process ($-\Delta G$, Table 1), which is calculated from the reduction potentials of the pyridinium, the oxidation potentials of the excited-state complexes and so forth. The k_q value correlates well with the $-\Delta G$ value, suggesting that the observed emission quenching originates in the electron transfer from the metal complex (*i.e.*, $[Ru(bpy)_3]^{2+}$ or $[Ir(ppy)_2(bpy)]^+$) in the excited state to pyridinium (*i.e.*, $\mathbf{2a}^+$, $\mathbf{5}^+$ or $\mathbf{6}^+$). It is worth noting that the electron transfer between $[Ir(ppy)_2(bpy)]^+$* to $\mathbf{6}^+$ is highly an endergonic process ($-\Delta G = -0.30$ eV) and, therefore, no emission quenching has been observed. Thus, an introduction of a nitro group(s) into a pyridinium skeleton improves the electron-accepting ability.

Conclusions

A combination of an electron-deficient pyridinium and electron-withdrawing nitro group(s) enhanced electron-accepting and oxidizing abilities. Each nitro-group introduction lowered the LUMO by several tenths of an electron volt, and dinitropyridinium $\mathbf{2a}^+$ especially served as an excellent oxidative quencher in photoinduced electron-transfer reactions. Since pyridinium derivatives have attracted increasing interest and utilized in a variety of photochemical systems such as natural/artificial photosynthesis, these nitropyridiniums are possible candidates as a new class of electron acceptors.

Author contributions

A. Ito: conceptulization, data curation, writing – original draft, and supervision. Y. Kuroda, K. Iwai and S. Yokoyama: investigation. N. Nishiwaki: supervision and writing – review & editing.

Conflicts of interest

There are no conflicts to declare.

Notes and references

1 J. A. Joule and K. Mills, *Heterocyclic Chemistry*, Wiley-Blackwell, New York, 5th edn, 2010.
2 A. Fulton and L. E. Lyons, *Aust. J. Chem.*, 1967, **20**, 2267; G. Unden and J. Bongaerts, *Biochim. Biophys. Acta*, 1997, **1320**, 217; J. Barber, *Chem. Phys. Rev.*, 2009, **38**, 185.
3 K. Kalyanasundaram, J. Kiwi and M. Grätzel, *Helv. Chim. Acta*, 1978, **61**, 2720; H. Misawa, H. Sakuragi, Y. Usui and K. Tokumaru, *Chem. Lett.*, 1983, **12**, 1021; A. Bose, P. He, C. Liu, B. D. Ellman, R. J. Twieg and S. D. Huang, *J. Am. Chem. Soc.*, 2002, **124**, 4; A. Ito, D. J. Stewart, Z. Fang, M. K. Brennaman and T. J. Meyer, *Proc. Natl. Acad. Sci. U.S.A.*, 2012, **109**, 15132; H. Yamamoto, M. Taomoto, A. Ito and D. Kosumi, *J. Photochem. Photobiol., A*, 2020, **401**, 112771.
4 D. Mauzerall and F. H. Westheimer, *J. Am. Chem. Soc.*, 1955, **77**, 2261; S. Fukuzumi, S. Koumitsu, K. Hironaka and T. Tanaka, *J. Am. Chem. Soc.*, 1987, **109**, 305; A. Kobayashi, H. Konno, K. Sakamoto, A. Sekine, Y. Ohashi, M. Iida and O. Ishitani, *Chem.–Eur. J.*, 2005, **11**, 4219; S. Ikeyama and Y. Amao, *ChemCatChem*, 2017, **9**, 833.
5 N. Nishiwaki and M. Ariga, *Top. Heterocycl. Chem.*, 2007, **8**, 43.
6 H. Asahara, M. Hamada, Y. Nakaike and N. Nishiwaki, *RSC Adv.*, 2015, **5**, 90778; Y. Nakaike, N. Nishiwaki, M. Ariga and Y. Tobe, *J. Org. Chem.*, 2014, **79**, 2163.
7 A. Ito, D. J. Stewart, Z. Fang, M. K. Brennaman and T. J. Meyer, *Proc. Natl. Acad. Sci. USA*, 2012, **109**, 15132; A. Ito, D. J. Stewart, T. E. Knight, Z. Fang,

M. K. Brennaman and T. J. Meyer, *J. Phys. Chem. B*, 2013, **117**, 3428; A. Ito, Z. Fang, M. K. Brennaman and T. J. Meyer, *Phys. Chem. Chem. Phys.*, 2014, **16**, 4880.

8 J. Sun, F. Zhong, X. Yi and J. Zhao, *Inorg. Chem.*, 2013, **52**, 6299.

9 Gibbs energy of photoinduced electron transfer, in *IUPAC Compendium of Chemical Terminology*, International Union of Pure and Applied Chemistry (IUPAC), 3rd edn, 2019, DOI: **10.1351/goldbook.GT07388**.

10 A. Ito and T. J. Meyer, *Phys. Chem. Chem. Phys.*, 2012, **14**, 13731.

11 M. J. Frisch, G. W. Trucks, H. B. Schlegel, G. E. Scuseria, M. A. Robb, J. R. Cheeseman, G. Scalmani, V. Barone, B. Mennucci, G. A. Petersson, H. Nakatsuji, M. Caricato, X. Li, H. P. Hratchian, A. F. Izmaylov, J. Bloino, G. Zheng, J. L. Sonnenberg, M. Hada, M. Ehara, K. Toyota, R. Fukuda, J. Hasegawa, M. Ishida, T. Nakajima, Y. Honda, O. Kitao, H. Nakai, T. Vreven, J. J. A. Montgomery, J. E. Peralta, F. Ogliaro, M. Bearpark, J. J. Heyd, E. Brothers, K. N. Kudin, V. N. Staroverov, R. Kobayashi, J. Normand, K. Raghavachari, A. Rendell, J. C. Burant, S. S. Iyengar, J. Tomasi, M. Cossi, N. Rega, J. M. Millam, M. Klene, J. E. Knox, J. B. Cross, V. Bakken, C. Adamo, J. Jaramillo, R. Gomperts, R. E. Stratmann, O. Yazyev, A. J. Austin, R. Cammi, C. Pomelli, J. W. Ochterski, R. L. Martin, K. Morokuma, V. G. Zakrzewski, G. A. Voth, P. Salvador, J. J. Dannenberg, S. Dapprich, A. D. Daniels, O. Farkas, J. B. Foresman, J. V. Ortiz, J. Cioslowski and D. J. Fox, *Gaussian 09 (Revision C.01)*, Gaussian, Inc., Wallingford, CT, 2009.

12 R. Dennington, T. Keith and J. Millam, *GaussView Version 5*, Semichem Inc., Shawnee Mission, KS, 2009.

13 J. N. Younathan, W. E. Jones and T. J. Meyer, *J. Phys. Chem.*, 1991, **95**, 488.

14 D. W. Thompson, A. Ito and T. J. Meyer, *Pure Appl. Chem.*, 2013, **85**, 1257.

15 A. Nakagawa, E. Sakuda, A. Ito and N. Kitamura, *Inorg. Chem.*, 2015, **54**, 10287.